Journal of Power Sources 275 (2015) 627–632

Contents lists available at ScienceDirect

Journal of Power Sources

journal homepage: www.elsevier.com/locate/jpowsour

Application of spouted bed elutriation in the recycling of lithium ion batteries

Daniel A. Bertuol [a, *], Camila Toniasso [a], Bernardo M. Jiménez [a], Lucas Meili [b], Guilherme L. Dotto [a], Eduardo H. Tanabe [a], Mônica L. Aguiar [c]

[a] Environmental Processes Laboratory (LAPAM), Chemical Engineering Department, Federal University of Santa Maria – UFSM, Santa Maria, RS, Brazil
[b] Chemical Engineering Department, Federal University of Alagoas – UFAL, Maceió, AL, Brazil
[c] Chemical Engineering Department, Federal University of São Carlos – UFSCAR, São Carlos, SP, Brazil

HIGHLIGHTS

- Application of Spouted Bed Elutriation in the recycling of LIB's.
- Efficient recovery of different materials present in LIB's.
- The materials are characterized and the recovery efficiencies determined.
- Physical and morphological properties of the particles are presented.
- Alternative process to separate the materials that compose spent LIB's.

ARTICLE INFO

Article history:
Received 9 September 2014
Received in revised form
21 October 2014
Accepted 8 November 2014
Available online 11 November 2014

Keywords:
Elutriation
Lithium–ion batteries
Spouted bed
Recycling

ABSTRACT

The growing environmental concern, associated with the continuous increase in electronic equipment production, has induced the development of new technologies to recycle the large number of spent batteries generated in recent years. The amount of spent lithium–ion batteries (LIBs) tends to grow over the next years. These batteries are composed by valuable metals, such as Li, Co, Cu and Al, which can be recovered. Thus, the present work is carried out in two main steps: In the first step, a characterization of the LIBs is performed. Batteries from different brands and models are dismantled and their components characterized regarding to the chemical composition and main phases. In the second step, a sample of LIBs is shredded and the different materials present are separated by spouted bed elutriation. The results show that spouted bed elutriation is a simple and inexpensive way to obtain the separation of the different materials (polymers, metals, active electrode materials) present in spent LIBs.

1. Introduction

The consumption and production of electronic and portable devices, associated with environmental issues, are the main generators of the use of rechargeable batteries. Among the different types of batteries, Li–ion batteries (LIBs) stand out due to their use in mobile phones. LIBs are preferred, once they are environmentally acceptable and efficient (i.e., having higher energy density, long cycle life, low self–discharge rate and safety in handling) [1]. There are two types of LIBs, primary and secondary. Primary batteries use metallic lithium, while secondary batteries are rechargeable and do not contain metallic lithium [2].

The structure of secondary LIBs is composed of a cathode, an anode, an organic electrolyte and a separator. The cathode is an aluminum plate coated with a mixture of cathodic active material, adhesives and additives. The anode consists of a copper plate coated with a mixture of graphite, adhesives and additives [2]. The composition varies slightly depending on the manufacturer [3].

LIBs have the following operating principle: the energy is stored by the movement of lithium ions from the cathode to the anode (charging) or vice versa (discharge process) according to the overall reaction in Eq. (1) [4]:

$$LiCoO_2 + 6C \leftrightarrow Li_{(1-x)}CoO_2 + C_6Li_x \quad (1)$$

* Corresponding author. Environmental Processes Laboratory (LAPAM), Chemical Engineering Department, Federal University of Santa Maria – UFSM, UFSM, 1000, Roraima Avenue, 97105-900, Santa Maria, RS, Brazil.
E-mail address: dbertuol@gmail.com (D.A. Bertuol).

http://dx.doi.org/10.1016/j.jpowsour.2014.11.036
0378-7753/

The cathodic active material most commonly used in LIBs is $LiCoO_2$. This material offers significant advantages regarding to synthesis, high working potential and excellent cycle ability at room temperature. In spite of this, alternatives have been developed to decrease costs and improve the stability [5,6]. The issue of the toxicity and cost of $LiCoO_2$ has been solved by opting for alternative transition metal oxide cathodes, such as, $LiNiO_2$ and $LiMnO_2$. $LiNiO_2$ is cheaper and has a higher energy density, but is less stable and less ordered as compared to $LiCoO_2$ [5,6]. On the other hand, $LiMnO_2$ has obtained results with considerable success as a viable metal oxide cathode [5].

Currently, the recycling of LIBs presents different processes and technologies proposed in the literature. These methods are based on physical and chemical processes. Among the physical processes, the highlighted are mechanical separation and thermal treatments. Regarding to the chemical processes acid leaching, bioleaching, solvent extraction, chemical precipitation and electrochemical treatments stand out [4]. Generally, better results are found by a combination of physical and chemical processes.

The mechanical separation processes are usually employed as a pre–treatment to promote the removal of the external casing, and to release and concentrate the metallic fraction, which will be sent to a hydrometallurgical or a pyrometallurgical process [7–11]. The operations normally used in mechanical separation are: magnetic and electrostatic separation, crushing, gravity separation, grinding, sieving, vibrating screen, pneumatic separation, air separation in zigzag classifier and flotation [3,10–14]. However, there is no information on the application of spouted bed elutriation in battery recycling.

This work focused on the separation of the different materials present in the LIBs, and was performed in two steps. In the first step, batteries of different brands and models were characterized regarding to the quantity of each material and its chemical composition. The second step comprised the application of mechanical methods (grinding, sieving and elutriation) to separate the different materials that compose LIBs. The spouted bed elutriation was used as a simple and cheap alternative for the separation of the different materials present in this kind of waste.

2. Materials and methods

2.1. LIBs characterization

Three different brands of batteries were used to quantify the materials present in the LIBs. The batteries were manually opened using tools, such as, pliers and scissors, and the different components were separated, classified and individually weighed (Shimadzu, AY 220). After the manual opening, batteries were weighed again and placed in an oven at 60 °C, until reach constant mass.

The characterization of the materials adhered onto the anode and cathode surfaces was performed by X–ray diffraction (Rigaku–Miniflex 300). The metals present in the batteries were identified by scanning electron microscopy (SEM), coupled with X–ray dispersive spectroscopy (EDS) (Philips, XL–30 FEG).

2.2. Mechanical processing

Fig. 1 shows the sequence of operations used in the mechanical processing and separation of the LIBs.

2.2.1. Grinding and sieving

The batteries were comminuted in a hammer mill (Tiger A4) with aperture of 10 mm. Then, the separation was carried out using a sieve with opening of 0.211 mm, and a sieve shaker (1st size separation in Fig. 1). Thus, the separation of metallic and polymeric fractions from the powder fraction constituted of $LiCoO_2$ and graphite occurred.

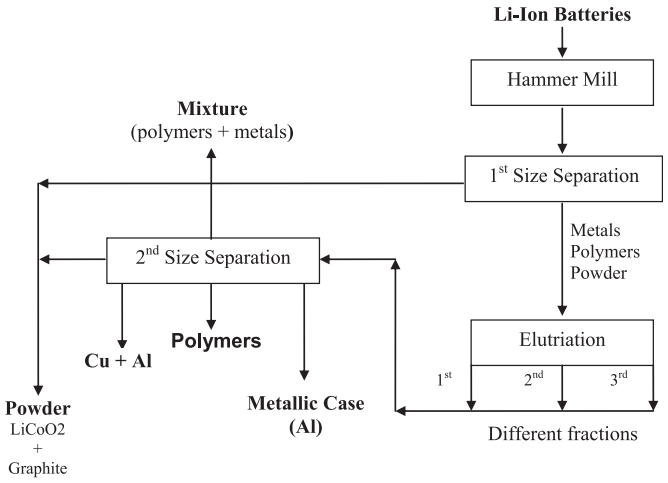

Fig. 1. Flow chart of the operations used in the mechanical processing.

2.2.2. Spouted bed elutriation

Fig. 2 shows the scheme of the spouted bed elutriation used in the experiments. The equipment consists of a cylindrical acrylic column, with a stainless steel conical base, and a Lapple cyclone coupled to the bed output. The bed dimensions are shown in Table 1.

The metallic and polymeric fractions (constituted by the external casing, copper, aluminum and polymers) and some powders that remained adhered to these fractions were fed in the spouted bed to perform the elutriation. The air flow was supplied by a radial blower (Artec, Model ACR 7.5) with 7.5 HP and maximum flow of 6.2 $m^3\ min^{-1}$. Air flow regulation was done by a potentiometer. The air velocity was measured by a thermo–anemometer propeller (Instruterm, CAS–500) with measurement range from 0 to 30 $m\ s^{-1}$ and accuracy of 0.1 $m\ s^{-1}$.

In the first elutriation stage (1st elutriation in Fig. 1), the drag of the polymer fraction, together with the smaller diameter particles of the aluminum and copper fraction (Cu/Al) and a small quantity of powder ($LiCoO_2$ and graphite), which was adhered to the surface of different particles, was carried out. In order to separate these fractions, it was necessary to perform a new sieving operation in a sieve shaker (2nd size separation in Fig. 1).

The remaining material in the bed underwent a second elutriation stage (2nd elutriation in Fig. 1) to withdraw the second fraction of Cu/Al particles of larger diameters. The obtained material was also sent to the sieving step with a sieve shaker (2nd size separation in Fig. 1), where it was possible to purify the Cu/Al fraction, and obtain two others fractions: a polymeric fraction and a fraction of mixed materials that should go back to the grinding step and then return to the process.

The last fraction, consisting basically of the LIBs external casing, was separated by increasing the air velocity in the bed inlet (V_f), until the last particle was dragged (3rd elutriation in Fig. 1). The air velocities (V_f) used in the bed inlet were from 1 $m\ s^{-1}$ to 21 $m\ s^{-1}$. All experiments were performed in triplicate ($n = 3$), and only the mean values were reported.

2.3. Characterization of the materials after separation

The materials separated after the sieving and elutriation steps were characterized to determine the physical and morphological

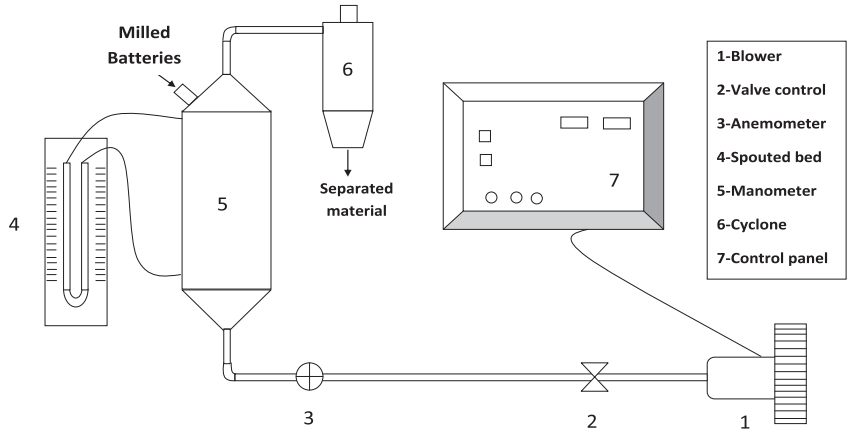

Fig. 2. Mounting scheme the spouted bed used in the elutriation.

properties of the particles. The volume (d_v), surface (d_S), Sauter (d_{SV}) and Stokes (d_{st}) diameters of the metallic and polymeric particles were obtained using a sieve shaker (Bertel). The specific mass of the particles was obtained using a digital Helium pycnometer (Micromeritics–Accupyc 1330).

The sphericity determination was performed from the particle diameters (minimum (r_{min}), medium (r_{mean}) and maximum (r_{max})), by Image Pro Plus 7.0 software. Images of the different separated fractions (polymers, external casing, Cu/Al) were obtained using a Galai Macro–Viewer illuminating table and a Sony XC–75 video camera. The particle sphericity ϕ was determined by shape factor, (S_f) and describes its three–dimensional variation (a particle is more spherical when the S_f value is closer to 0) [15]. The calculation of particle shape factor was made by the Eqs. (2–5) [16–18]:

$$r_{mean} = \frac{\sum_{i=1}^{n} r_i}{n} \tag{2}$$

$$r_{rms\cdot d} = \sqrt{\frac{(r_{\max} - r_{mean})^2 + (r_{\min} - r_{mean})^2}{2}} \tag{3}$$

$$S_f = \frac{r_{rms\cdot d}}{r_{mean}} \tag{4}$$

$$\phi = 1 - S_f \tag{5}$$

where, r_{mean} is the mean diameter (m), $r_{rms\cdot d}$ is the of root mean square (RMS) deviation (m), $r_{\min}$ is the minimum diameter (m), $r_{\max}$ is the maximum diameter (m). The diameters (r_{mean}, $r_{\min}$, $r_{\max}$) were determined by analyzing the images obtained with an optical microscope with the Image Pro Plus 7.0. software. This methodology was used for metal and powder particles.

Table 1
Characteristic dimensions of the spouted bed apparatus.

Characteristics	Dimensions (cm)
Column diameter	17.0
Height of bed	54.0
Cone bottom diameter	0.2
Height of lower cone	14.0
Diameter of upper cone	7.0
Height of upper cone	7.0
Diameter of cyclone cylindrical section	15.0
Height of cyclone	27.0

The polymers sphericity was determined by the Mohsenin methodology [19], considering that the particles had a more planar shape, as presented in Eq. (6):

$$\phi = \frac{(lw\delta)^{1/3}}{l} \tag{6}$$

where, l, w and δ are respectively, the length, width and thickness (m) of the material, and $(lw\delta)^{1/3}$ is the particle geometrical deviation.

To find the terminal velocity (u_t), two dimensionless quantities were defined. A dimensionless terminal velocity (u^*) (Eq. (7)) and a dimensionless particle diameter d^* (Eq. (8)) as follows [18]:

$$u_* = u_t \left[\frac{\rho_f^2}{g u \left(\rho_s - \rho_f\right)}\right]^{\frac{1}{3}} \tag{7}$$

$$d_* = d_{sph} \left[\frac{g\rho_f \left(\rho_s - \rho_f\right)}{\mu^2}\right]^{\frac{1}{3}} \tag{8}$$

where, u_t is the terminal velocity (m s^{-1}), d_{sph} is the equivalent spherical diameter (m), ρ_f is the fluid specific mass (kg m^{-3}), ρ_p is the particle specific mass (kg m^{-3}), g is the gravity acceleration (m s^{-2}) and μ the viscosity (kg m^{-1} s^{-1}).

The correlation to predict the terminal velocities for isometric particles, given the information on the particles and physical properties of the fluid, may be approximated by Eq. (9) [20]:

$$u^* = \left[\frac{18}{d_*^2} + \frac{(2.3348 - 1.7439\varphi)}{d_*^{0.5}}\right]^{-1} \quad 0.5 \le \phi \le 1 \tag{9}$$

3. Results and discussion

3.1. LIBs characterization

3.1.1. Manual opening characterization

The batteries used in this work presented a prismatic form and were composed of an external casing with negative and positive electrodes and also the separators. The electrodes were comprised of a metallic leaf coated with the active materials ($LiCoO_2$ and

Table 2
Percentage of the different materials that composes the LIB's.

Material	Battery 1		Battery 2		Battery 3	
	Mass[a] (g)	Wt%	Mass[a] (g)	Wt%	Mass[a] (g)	Wt%
External case	2.60 ± 0.10	15.93	2.40 ± 0.10	14.23	3.21 ± 0.10	16.60
Copper	1.30 ± 0.10	7.97	1.20 ± 0.10	7.11	1.20 ± 0.1	6.20
Graphite	3.40 ± 0.10	20.83	3.00 ± 0.10	17.78	4.30 ± 0.20	22.23
Aluminum	1.50 ± 0.10	9.19	1.50 ± 0.10	8.89	0.74 ± 0.10	3.83
$LiCoO_2$	4.10 ± 0.20	25.12	4.90 ± 0.20	29.05	5.35 ± 0.20	27.66
Polymers	1.90 ± 0.10	11.64	2.05 ± 0.10	12.15	2.22 ± 0.10	11.48
Electrolyte	1.52 ± 0.10	9.31	1.82 ± 0.10	10.79	2.32 ± 0.10	12.00

[a] Mean ± standard error ($n = 3$).

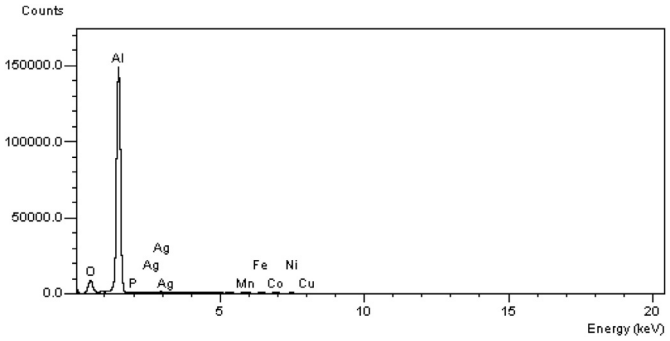

Fig. 3. EDS spectrum of the external case.

graphite) in powder form [21]. The batteries' compounds were manually separated and classified as: external casing, Cu, Al, $LiCoO_2$, polymers, graphite and electrolytes. The results (in weight basis) regarding of the batteries characterization are show in Table 2. Table 2 shows that $LiCoO_2$ was the main component of the batteries, with about 30 wt% of the total mass, and that graphite constituted about 20 wt% of the total mass was [14].

3.1.2. SEM, EDS and XRD

The SEM and EDS of the different materials were performed after the manual separation. According to the energy dispersive spectroscopy (EDS) analysis showed in Fig. 3, the external casing is basically made up of aluminum [10]. The remaining components are possibly associated with some surface contamination because the external casing suffered no pretreatment.

Figs. 4 and 5 show, respectively, the chemical composition of the $LiCoO_2$ and the graphite supports. Figs. 4 and 5 confirm that the $LiCoO_2$ support is mainly constituted by Al, and that the graphite support is mainly constituted by Cu [10].

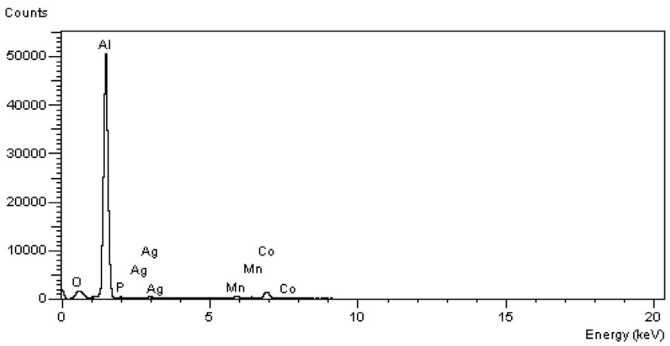

Fig. 4. EDS spectrum of the $LiCoO_2$ metallic support.

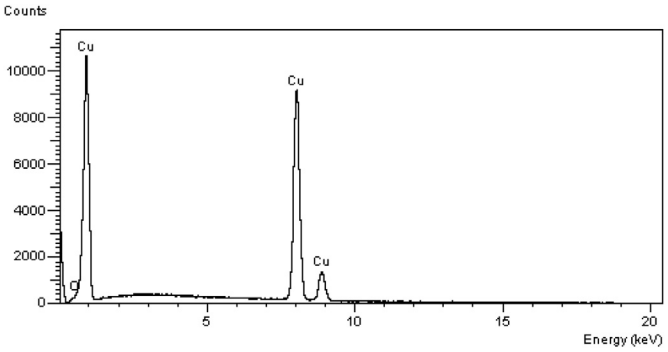

Fig. 5. EDS spectrum of the graphite metallic support.

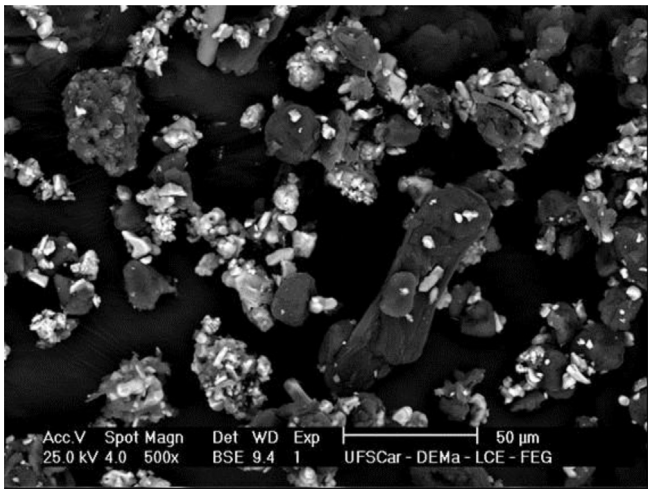

Fig. 6. SEM images of the electrode materials of spent LIB's.

Fig. 6 shows the SEM images of $LiCoO_2$ and graphite particles. Two distinct particle groups can be seen in Fig. 6. The larger particles can be attributed to graphite and the smaller particles can be attributed to $LiCoO_2$ [22].

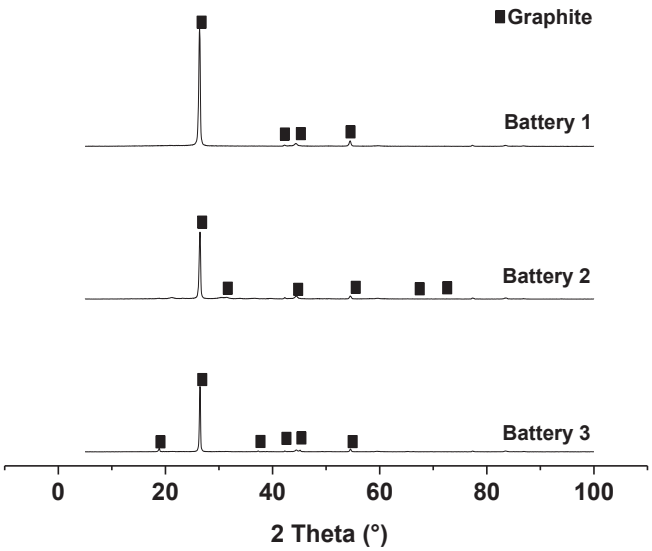

Fig. 7. XRD patterns of the battery anode.

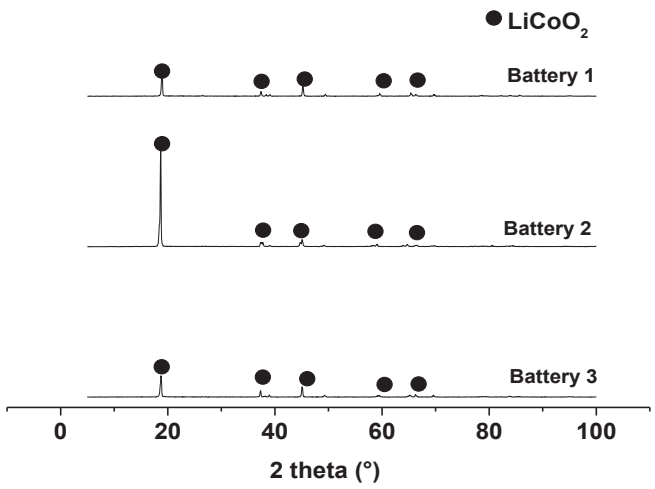

Fig. 8. XRD patterns of the battery cathode.

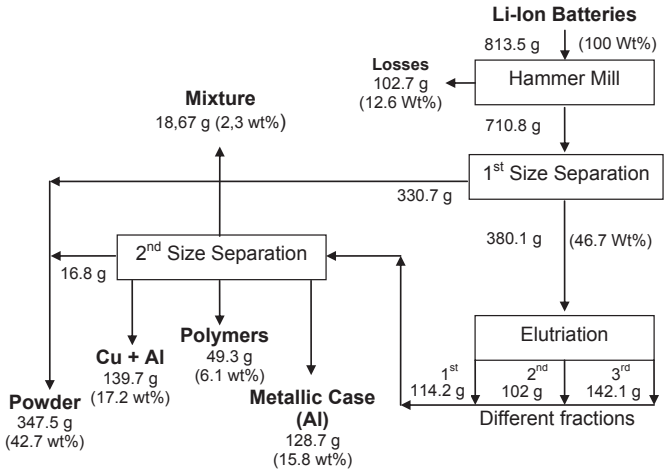

Fig. 9. Final mass balance of LIB's mechanical processing.

For all batteries, the XRD patterns were similar. The results confirmed that the anodic material is graphite, while the cathodic material is $LiCoO_2$ (Figs. 7 and 8).

3.2. Mechanical processing and separation

Fig. 9 shows the final mass balance of mechanical processing and separation of LIBs. The mechanical processing was performed with 40 batteries, which represents an initial mass of 813.5 g. These batteries were ground in a hammer mill for the mechanical size reduction. After this operation, the mass was reduced to 710.8 g, representing a loss of 12.6 wt% in relation to the initial mass. Since that, the electrolytes represent about 10 wt% of the total mass (as presented in Table 2) and were volatilized in the process [4], the losses in this step, discounting the volatilized electrolytes, were only 2.6 wt%. This loss of 2.6 wt% is associated with the material retained in the mill during milling.

After the grinding step, the material was sieved in order to separate the powder fraction from the other materials. This step provided 330.7 g of powder ($LiCoO_2$ and graphite) and 380.1 g of the other materials (external casing, Al, Cu, polymers and adhered waste powder).

The above-mentioned 380.1 g were submitted to spouted bed elutriation (Fig. 2). In the spouted bed elutriation, the materials were exposed to different air velocities, and consequently, the fractions were separated by specific mass and particle size differences. The first fraction (polymers, Cu and Al with smaller diameters) was dragged at air velocities of about 10.2–10.5 m s^{-1}, and then separated by sieving. This fraction was composed by 38.46 g of polymers (diameter larger than 6.7 mm), 57.9 g of Cu plus Al (diameter larger than 0.6 mm and smaller than 6.7 mm) and 17.84 g of powder (diameter smaller than 0.211 mm), totalizing 114.2 g of material.

Afterward, with the material remaining in the bed, the second fraction (Cu and Al with higher diameters plus a metal/polymers mixture) was dragged at air velocities of 10.6–13.0 m s^{-1}, and then separated by sieving. This fraction was composed of 18.67 g of a metal and polymers mixture with diameter larger than 6.7 mm; 0.545 g of polymers, with diameter between 6.7 and 4.75 mm; and 82.78 g of Cu and Al with diameter smaller than 4.75 mm, totalizing 102 g of material.

Finally, with the last material remaining in the bed, the third fraction with 142.1 g of aluminum external casing was dragged at air velocities of 13.0–20.7 m s^{-1}. In the steps of elutriation and sieving, the losses were 3.3 wt% in relation to the initial mass. This loss is associated with the material that was retained in the equipments.

3.3. Characterization of the fractions obtained after the mechanical processing

Fig. 10 shows the images (obtained using an optical microscope) of the three different fractions obtained in the mechanical processing. These different fractions were characterized and the results are shown in Tables 3 and 4.

The experimental inlet air velocities (V_f) were compared with the theoretical terminal velocities of the isolated particles (u_t). For this purpose Eqs. (7–9) were employed and the Stokes diameter (d_{st}) was considered. The V_f and u_t values for each particle are

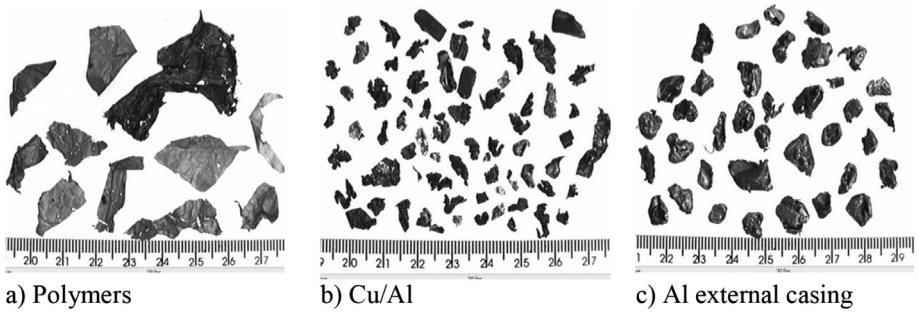

Fig. 10. Optical images of the particulate materials obtained after the spouted bed elutriation.

Table 3
Specific mass and diameters for the different fractions.

Material	ρ(g/cm^3)	d_v (mm)	d_s(mm)	d_{sv} (mm)	d_{St} (mm)
1st polymers fraction	1.66	5.84	5.43	6.75	6.05
1st Cu/Al fraction	3.15	1.64	1.44	2.11	1.74
2nd Cu/Al fraction	3.11	2.49	2.27	3.01	2.61
3rd aluminum fraction	2.92	4.46	4.29	4.82	4.55

Table 4
Sphericity of the different fractions.

Material	r_{min}(mm)	r_{max} (mm)	r_{mean} (mm)	S_f(−)	ϕ
1st polymers fraction	7.40 ± 3.80	19.90 ± 9.90	16.60 ± 7.50	–	0.14
1st Cu/Al fraction	1.50 ± 0.80	4.00 ± 3.50	2.60 ± 1.30	0.46	0.54
2nd Cu/Al fraction	2.70 ± 1.10	6.60 ± 2.80	4.70 ± 1.40	0.51	0.59
3rd aluminum fraction	4.60 ± 1.30	9.40 ± 6.10	6.60 ± 2.00	0.36	0.64

Table 5
Comparison between the inlet air velocities and terminal velocities.

Material type	u_t (m/s)	V_f (m/s)
1st fraction A (Polymers)	4.54	10.20–10.50
1st fraction B (Cu + Al)	4.78	10.20–10.50
2nd fraction (Cu + Al)	6.25	10.60–13.00
3rd fraction (Aluminum)	8.61	13.10–20.70

shown in Table 5. The results in Table 5 demonstrated that the first fraction (polymers, Cu and Al with smaller diameters) was dragged at lower V_f values, since the u_t was lower. When V_f was increased, the second and third fractions were successively separated, due to its different u_t values. It was found in Table 5, that $V_f > u_t$. This behavior can be explained on the basis of the fluid dynamic behavior of the spouted bed.

Spouted beds are roughly divided into three different regions, each with its own specific flow behavior: the annulus, the spout and the fountain, as shown in Fig. 11 [20]. Particles are carried up by gas in the spout, reach the top of the bed and form a fountain and then drop down due to gravity, and move downward though the annulus. Thus, the motion of the particles in the spout, annulus and fountain zones forms a circulation of particles in the bed [23]. Shuyan et al. [24], Olazar et al. [25] and Béttega et al. [23], studied the velocity profiles of the particles in the spout region. They verified that the vertical component of the particle velocity in the spout reaches a maximum value near the bottom at a radial position $r = 0$. However, the velocity decreases, when the particles move in the axial direction. Thus, it can be affirmed that a higher V_f is required in relation to u_t, in order to compensate the energy losses that occurs during the particle movement in the axial direction. Finally, it was verified that the separation of the different components of the batteries can be successfully performed by spouted bed elutriation.

4. Conclusion

The mechanical processing was efficient to separate the different materials that compose the LIBs (electrode active materials, polymers, Cu and Al). From the mechanical processing, it was possible to separate the materials as: 17.2 wt% of Cu/Al, 15.8 wt% of Al (external casing); 42.7 wt% of $LiCoO_2$ and graphite, 6.1 wt% of polymers and 2.3 wt% of a mixture that can be reprocessed.

Using mechanical processing operations (grinding and sieving) and spouted bed elutriation, fractions that can be used by the recycling industries or directly commercialized in the market, were obtained. It was found that the spouted bed elutriation can be successfully employed as a viable and easy alternative to separate the materials that compose the spent LIBs.

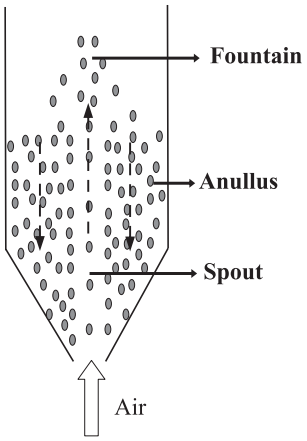

Fig. 11. Scheme of a conventional spouted bed operating in stable condition.

Acknowledgments

The authors wish to thank Capes, CNPq and Fapergs for the financial support to this work.

References

[1] X. Zhang, Y. Xie, H. Cao, F. Nawaz, Y. Zhang, Waste Manag. 34 (2014) 1715–1724.
[2] P. Zhang, T. Yokoyama, O. Itabashi, T.M. Suzuki, K. Inoue, Hydrometallurgy 47 (1998) 259–271.
[3] M.S. Shin, N.H. Kim, J.S. Sohn, D.H. Yang, Y.H. Kim, Hydrometallurgy 79 (2005) 172–181.
[4] J. Xu, H.R. Thomas, R.W. Francis, K.R. Lum, J. Wang, B. Liang, J. Power Sources 177 (2008) 512–527.
[5] R. Mukherjee, R. Krishnan, T.M. Lu, N. Koratkar, Nano Energy 1 (2012) 518–533.
[6] V.M. Mohan, B. Hu, W. Qiu, W. Chen, J. Appl. Electrochem. 39 (2009) 2001–2006.
[7] C. Lupi, M. Pasquali, A. Dell'Era, Waste Manag. 25 (2005) 215–220.
[8] L. Sun, K. Qiu, Waste Manag. 32 (2012) 1575–1582.
[9] D.A. Bertuol, A.M. Bernardes, J.A.S. Tenório, J. Power Sources 60 (2006) 465–1470.
[10] Y. Zhang, Y. He, F. Wang, L. Ge, X. Zhu, H. Li, Waste Manag. 34 (2014) 1051–1058.
[11] S. Al–Thyabat, T. Nakamura, E. Shibata, A. Iizuka, Miner. Eng. 45 (2013) 4–17.
[12] K. Huang, J. Li, Z. Xu, Waste Manag. 31 (2011) 1292–1299.
[13] E. Gratz, Q. Sa, D. Apelian, Y. Wang, J. Power Sources 262 (2014) 255–262.
[14] T. Georgi–Maschler, B. Friedrich, R. Weyhe, H. Heegn, M. Rutz, J. Power Sources 207 (2012) 173–182.
[15] Y.K. Yen, C.L. Lin, J.D. Miller, Powder Technol. 98 (1998) 1–12.
[16] R.M. Carter, Y. Yan, J. Phys. Conf. Ser. 15 (2005) 177–182.
[17] C.W. Liao, J.H. Yu, Y.S. Tarng, Particulogy 8 (2010) 286–292.
[18] A.L. Chen, B.Z. Chen, A. Feng, Adv. Powder Technol. 25 (2014) 508–513.
[19] N.N. Mohseninn, Physical Properties of Plant and Animal Materials, Gordon and Breach Science Publishers, New York, 1980.
[20] A. Haider, O. Levenspiel, Powder Technol. 58 (1989) 63–70.
[21] M.K. Jha, A. Kumari, A.K. Jha, V. Kumar, J. Hait, B.D. Pandley, Waste Manag. 33 (2013) 1890–1897.
[22] T. Zhang, Y. He, L. Ge, R. Fu, X. Zhang, Y. Huang, J. Power Sources 240 (2013) 766–771.
[23] R. Béttega, R.G. Corrêa, J.T. Freire, Dry. Technol. 28 (2010) 1266–1276.
[24] W. Shuyan, L. Xiang, L. Huilin, Y. Long, S. Dan, H. Yurong, D. Yonglong, Powder Technol. 196 (2009) 184–193.
[25] M. Olazar, M.J. San José, M.A. Izquierdo, A.O. Salazar, J. Bilbao, Chem. Eng. Sci. 56 (2001) 3585–3594.